



## *Supplement of*

# **Interpreting eddy covariance data from heterogeneous Siberian tundra: land-cover-specific methane fluxes and spatial representativeness**

**J.-P. Tuovinen et al.**

*Correspondence to:* Juha-Pekka Tuovinen ([juha-pekka.tuovinen@fmi.fi](mailto:juha-pekka.tuovinen@fmi.fi))

The copyright of individual parts of the supplement might differ from the CC BY 4.0 License.

## S1. Footprint analysis

The flux footprint defined by Eq. (1) in the main text provides a means to identify and depict the influence of a two-dimensional ground source on a point measurement. However, there are alternative ways of doing this, some of which are formalized here for clarity. Following Schmid (1994), we first define the cumulative footprint, or the source area,  $\Pi$ , in such a way that it corresponds to the smallest bounded region containing the surface elements that contribute to the measurement signal by a specified fraction  $P \in (0,1)$ . The source area defined in this way is bounded by a footprint isopleth,  $f = f_P$ , within which the integral of  $f$  equals  $P$ ,

$$\Pi(f_P) = \int_0^{2\pi} \left( \int_{r_{P,1}(\theta)}^{r_{P,2}(\theta)} f(\theta, r) dr \right) d\theta = P, \quad (\text{S1})$$

where the direction-dependent distances  $r_{P,1}(\theta)$  and  $r_{P,2}(\theta) > r_{P,1}(\theta)$  are defined by the condition  $f > f_P$ , if  $r_{P,1} < r < r_{P,2}$ . This formulation defines an arbitrary area, but it is also possible to derive averaged dimensions in terms of a direction-independent range  $r_{P,1} - r_{P,2}$ , i.e., an annulus, corresponding to a given  $P$ , if we first integrate along the angular coordinate,

$$\Pi^*(r_{P,1}, r_{P,2}) = \int_{r_{P,1}}^{r_{P,2}} \left( \int_0^{2\pi} f(\theta, r) d\theta \right) dr = P, \quad (\text{S2})$$

where the distances  $r_{P,1}$  and  $r_{P,2}$  minimize the annular area. (It is assumed here that the footprint distribution makes it possible to define unique  $r_{P,1}$  and  $r_{P,2}$ , which is not true for an arbitrary  $f$ ). Both Eqs. (S1) and (S2) mean that also the closest edge of the source area, i.e.,  $r_{P,1}$ , is located at a distance upwind from the measurement point. While Eq. (S1) answers the question “*What is the area that contributes most to the measured flux?*”, Eq. (S2) corresponds to “*From which range does the flux originate, on average?*”

Alternatively, we can set  $r_{P,1} = 0$  and define the cumulative footprint corresponding to Eqs. (S1) and (S2) as

$$\Pi_0(f_P) = \int_0^{2\pi} \left( \int_0^{r_P(\theta)} f(\theta, r) dr \right) d\theta = P \quad (\text{S3})$$

and

$$\Pi_0^*(r_P) = \int_0^{r_P} \left( \int_0^{2\pi} f(\theta, r) d\theta \right) dr = P, \quad (\text{S4})$$

respectively. In Eq. (S3), the distance  $r_P(\theta)$  coincides with a footprint isopleth. These definitions make it possible to characterize the measurement with a distance that is related to the traditional fetch concept (Dyer, 1963).

The area of influence is also commonly depicted on the basis of the cross-wind integrated footprint, where the integration is performed in Cartesian coordinates simply as

$$\Pi_C(f_P) = \int_0^{x_P} \left( \int_{-\infty}^{\infty} f(x, y) dy \right) dx = P, \quad (\text{S5})$$

where  $x_P$  is the distance from the mast within which the proportion  $P$  of the measured flux originates from, termed the “effective fetch” by Gash (1986). This is a useful definition if  $f$  represents stationary conditions, i.e., a single short-term

period, while  $\Pi$ ,  $\Pi^*$ ,  $\Pi_0$  and  $\Pi_0^*$  can be meaningfully determined also for the footprint averaged over multiple flow conditions, i.e., for the time-averaged  $f$  representing a footprint climatology.

To illustrate the expected range of flux footprint distributions of the EC measurements at Tiksi, Table S1 presents characteristic source area dimensions calculated with the meteorological data detailed in Table 2 in the main text according to different source area definitions above: a full three-dimensional footprint,  $\Pi$  (Eq. S1), for a single, arbitrary wind direction; the corresponding cross-wind integrated footprint,  $\Pi_C$  (Eq. S5); and an annular footprint climatology,  $\Pi^*$  (Eq. S2), calculated assuming an equal frequency of wind directions (in which case  $\Pi^*$  equals  $\Pi$ ).

Table S1 demonstrates expected qualitative features of flux footprints: the source areas are extensive over the aerodynamically smooth tundra terrain, and their dimensions increase with increasing atmospheric stability and with the proportional contribution to the measured flux,  $P$  (Schmid, 1994). While the distance of maximal surface influence in a single footprint varies by a factor of 2 ( $r_{\max} = 18\text{--}35$  m), depending on stability, for the estimated far end of the source area contributing 90 % to the flux this factor is almost 20 ( $r_{P,2} = 200\text{--}3500$  m). For the annular climatology, the dimensions are somewhat smaller (Table S1). It is noteworthy that variation in the efficiency of horizontal diffusion also plays a marked role in the spatial weighting of different surface elements and that the results for the cross-wind integrated footprint are not identical to those for the three-dimensional function; however, they are similar to the dimensions of the annular climatology. If the integration for the climatology case is started at the EC tower ( $\Pi_0$  and  $\Pi_0^*$ ), the resulting distance will be very close to  $r_{P,2}$  (results not shown). Overall, these results indicate that, when reporting dimensions of the area of influence, it is important to state the definition adopted for this source area.

## References

- Dyer, A. J.: The adjustment of profiles and eddy fluxes, Q. J. Roy. Meteor. Soc., 89, 276–280, 1963.
- Gash, J. H. C.: A note on estimating the effect of a limited fetch on micrometeorological evaporation, Bound.-Lay. Meteorol., 35, 409–413, 1986.
- Schmid, H. P.: Source area for scalars and scalar fluxes, Bound.-Lay. Meteorol., 67, 293–318, 1994.

Table S1. Source area dimensions for the example cases specified in Table 2 in the main text, calculated according to different definitions: (1) Single three-dimensional footprint  $\Pi$ ; (2) Single cross-wind integrated footprint  $\Pi_C$ ; and (3) Annular footprint climatology  $\Pi^*$ .

Case <sup>a</sup>	$P = 25 \%$	$P = 50 \%$	$P = 75 \%$	$P = 90 \%$	
(1) Single three-dimensional ( $\Pi$ )					
	$r_{\max}$ (m)	$r_{P,1} - r_{P,2}$ [max. width] <sup>b</sup> (m)			
Unstable	18	10–37 [12]	8–59 [21]	6–107 [40]	5–206 [74]
Neutral	27	13–75 [22]	9–143 [45]	7–338 [102]	5–915 [247]
Stable	35	15–126 [33]	10–287 [76]	7–897 [206]	5–3545 [652]
(2) Single cross-wind integrated ( $\Pi_C$ )					
	$r_{\max}$ (m)	$x_P$ (m)			
Unstable	23	27	46	86	168
Neutral	39	56	112	269	734
Stable	53	94	223	706	2805
(3) Annular climatology ( $\Pi^*$ )					
	$r_{\max}$ (m)	$r_{P,1} - r_{P,2}$ (m)			
Unstable	18	11–29	8–47	6–87	5–170
Neutral	26	14–57	10–113	7–272	5–740
Stable	34	16–95	11–225	7–711	5–2816

<sup>a</sup> Symbols:  $P$  = proportion of the measured flux originating from the surface elements within the dimensions indicated;

$r_{\max}$  = distance of the footprint maximum;  $r_{P,1}, r_{P,2}$  = distances between which the surface elements with the largest contribution to  $P$  are located;  $x_P$  = distance integrated from the EC tower location within which  $P$  originates from.

<sup>b</sup> Maximum width of the source area.

## Supplementary figures

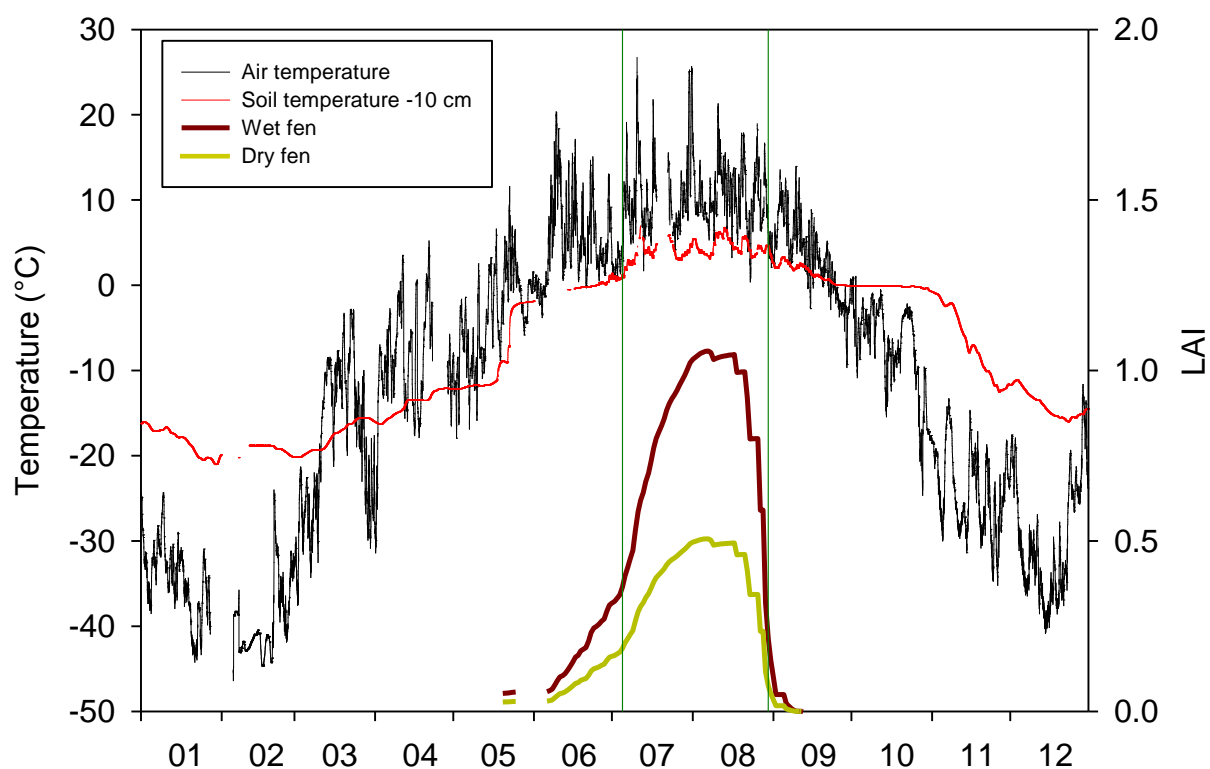


Figure S1. Air temperature, soil temperature at 10 cm depth in dry fen and the leaf area index (LAI) of the vascular plants on fens (Juutinen et al., 2017) at Tiksi in 2014. The vertical lines indicate the study period of 5 July to 29 August selected according to the thermal growing season (daily mean air temperature higher than 5 °C).

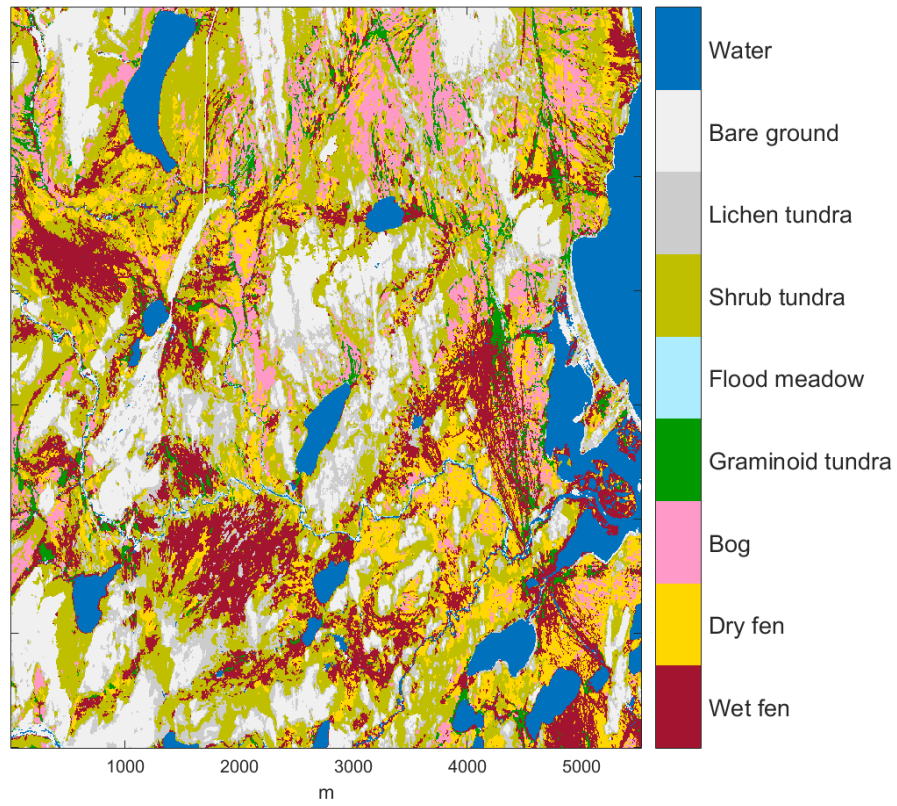


Figure S2. Land cover classification within the regional upscaling area of 35.8 km<sup>2</sup>.

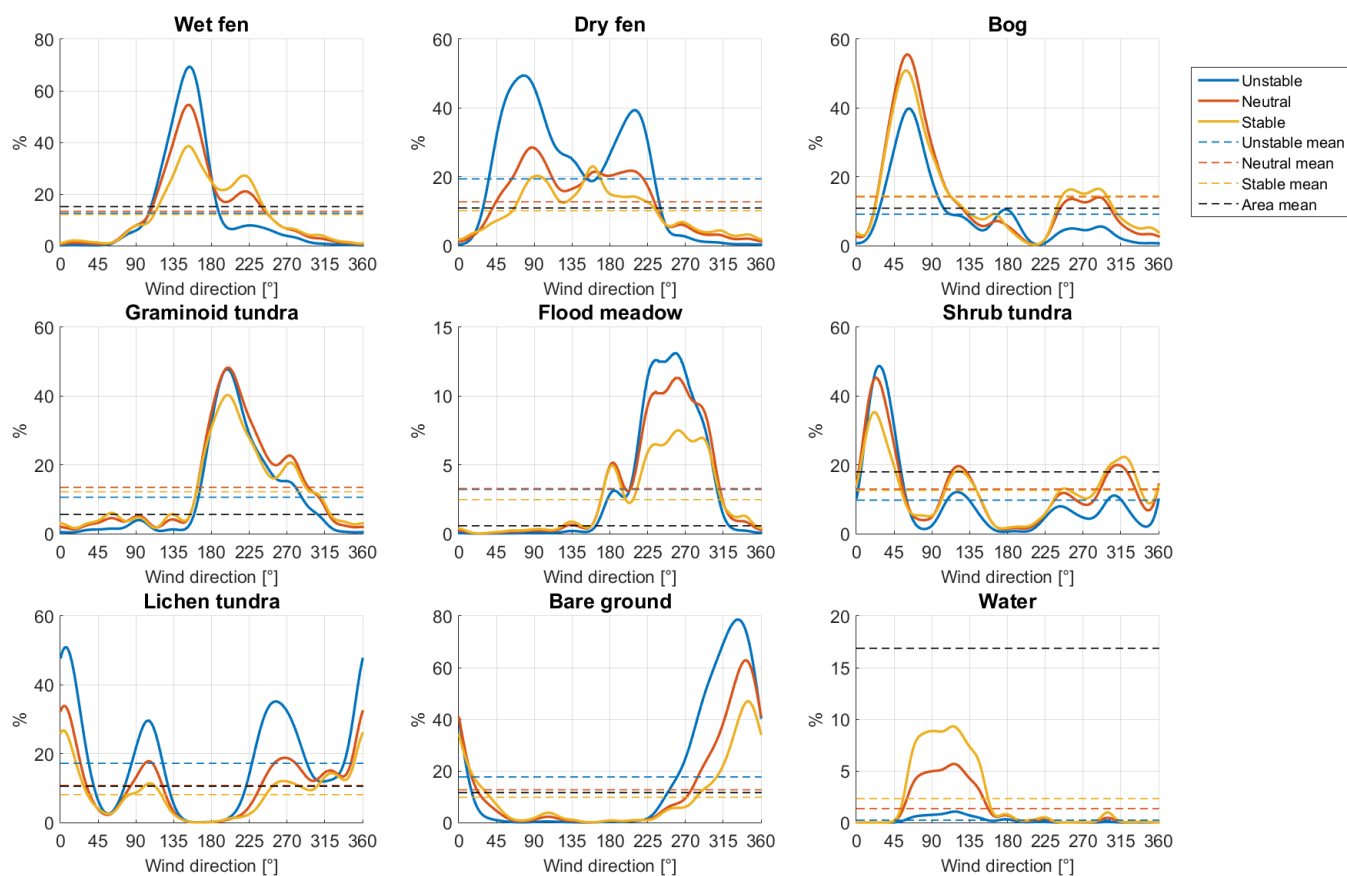


Figure S3. The footprint-weighted and area-averaged proportions of different land cover classes as a function of wind direction for the three flow conditions specified in Table 2.

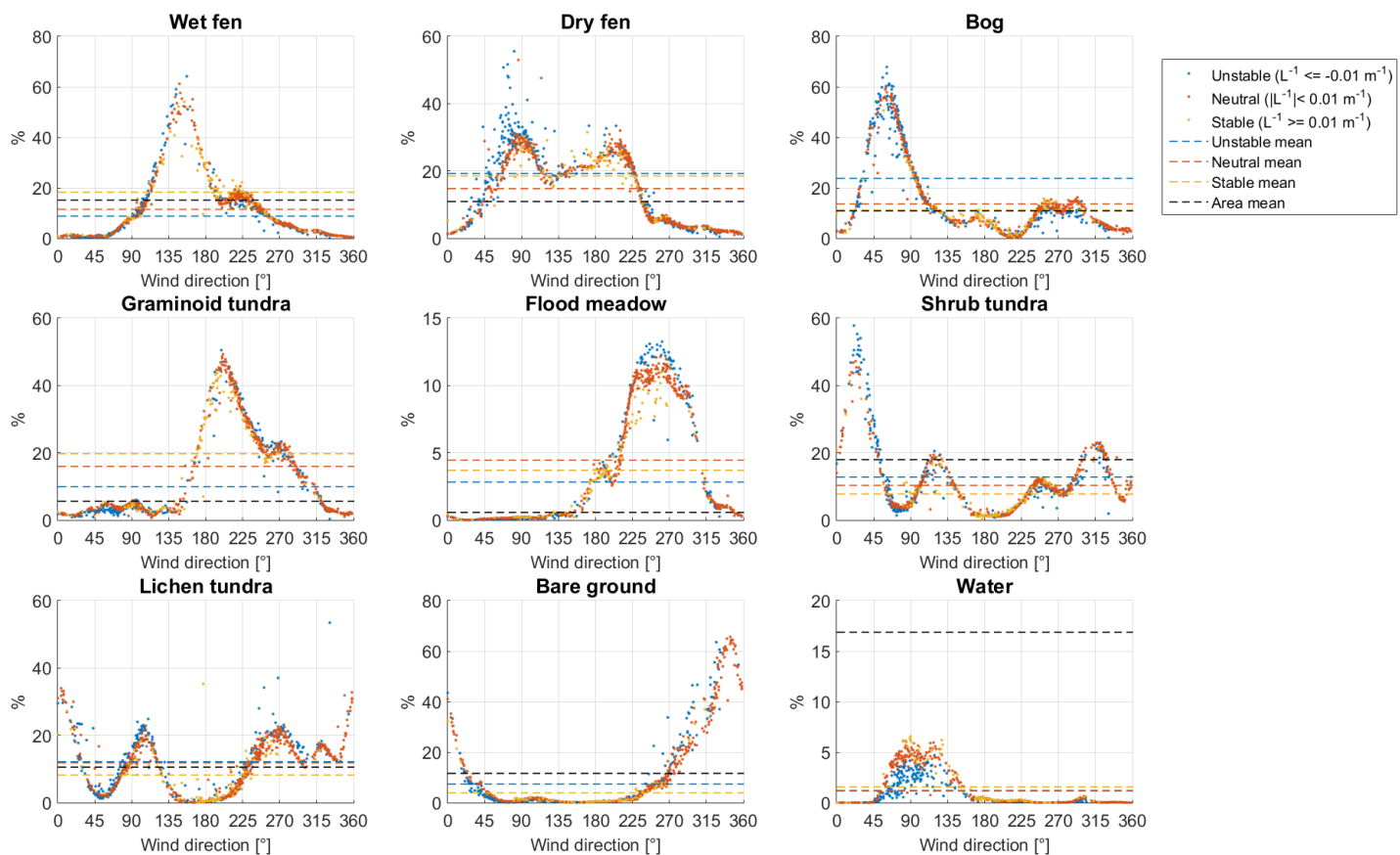


Figure S4. The footprint-weighted and area-averaged proportions of different land cover classes as a function of wind direction during the growing season of 2014.



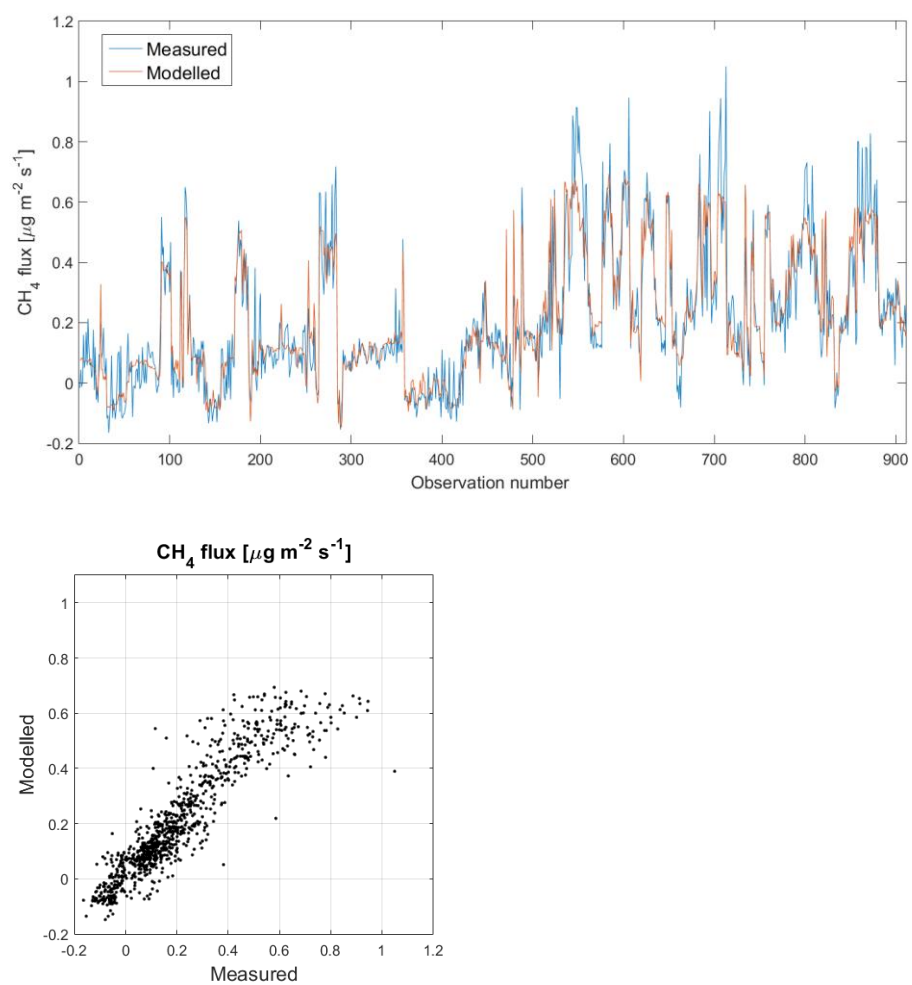


Figure S5. Half-hourly measured and modelled  $\text{CH}_4$  fluxes from 5 July to 29 August 2014. For clarity, the data gaps are removed, and thus the top panel does not depict a continuous time series.